Journal of Zhejiang University-SCIENCE A (Applied Physics & Engineering)
ISSN 1673-565X (Print); ISSN 1862-1775 (Online)
www.zju.edu.cn/jzus; www.springerlink.com
E-mail: jzus@zju.edu.cn

Wrinkle analysis of a space planar film reflect-array*

Wei-wei XIAO, Wu-jun CHEN†‡, Gong-yi FU

(*Space Structures Research Centre, Shanghai Jiao Tong University, Shanghai 200030, China*)

†E-mail: cwj@sjtu.edu.cn

Received June 1, 2010; Revision accepted Sept. 1, 2010; Crosschecked Dec. 10, 2010

Abstract: The presence of wrinkles in a membrane is the main factor that induces surface errors on space planar film reflect-arrays. Based on the commercial finite element (FE) package ABAQUS, a numerical procedure for membrane wrinkle analysis was set up, and used to analyze a square planar film reflect-array under pure shear force to evaluate its induced wrinkle characteristics. First, the effect of shear force on the wrinkle pattern of the array was studied and validated by experiment. Second, the effect of prestress was studied. When the prestress increases, the quantity of the wrinkles increases, and the amplitude of the wrinkles decreases. Third, the influence of the boundary conditions was investigated. A frame side edge structure has a relatively smooth surface, but also relatively high stress. Finally, the behavior of a joint seam was analyzed. The results indicate that a joint band has a significant influence on the wrinkle pattern of the membrane.

Key words: Space planar film reflect-array, Wrinkle analysis, Joint seam
doi:10.1631/jzus.A1000257 **Document code:** A **CLC number:** V214; O312

1 Introduction

There has been increasing interest in the application of membrane structures in space, such as in inflation antennas, space telescope optics, solar sails and synthetic aperture radar. Folding and compression of these membrane structures during manufacture and packaging can produce wrinkles in the membrane. The presence of wrinkles in membranes is the main cause of surface errors in precision space membrane structures. Such errors restrict their technical function and performance, because the efficiency of these membrane structures depends on the geometric accuracy of their surfaces. In some applications, a membrane with a small, known winkle pattern can be acceptable. Thus, it is important to predict the size and configuration of such wrinkles, to ensure that the surface geometry maintains the structure's performance (Calladine, 1983; Steigmann and Pipkin, 1989a; 1989b; Greschik and Mikulas, 2001; Lai, 2001).

There have been many studies of membrane wrinkling both on an analytical basis and using numerical simulation. Stein and Hedgepeth (1961) carried out a theoretical analysis of partly wrinkled membranes. Mansfield (1968; 1970) developed the famous tension field theory and analyzed a wrinkled membrane's load transfer. Pipkin (1986) studied the relaxed energy density of an isotropic elastic membrane. These theoretical solutions were applicable mainly to simple boundary conditions.

With advances in nonlinear computational methods and computer-aided technology, the simulation of highly complicated nonlinear geometrical wrinkled deformations in thin membranes recently became possible. A finite element method (FEM), named the iterative membrane properties method (IMP), that incorporates wrinkle theory was introduced by Miller and Hedgepeth (1985) and extended by Adler and Mikulas (2000) to implement a user subroutine to define a material's mechanical behavior in several commercial FE packages, e.g., ABAQUS and NASTRAN. Johnston (2002) used this ABAQUS

‡ Corresponding author
* Project (Nos. 50878128 and 50808122) supported by the National Natural Science Foundation of China

subroutine to analyze the static and dynamic behavior of a one-tenth scale sunshield. Mseikeh (1997) used the dynamic relaxation method and a triangular shell element to analyze the gravity-induced wrinkling of a blanket and the wrinkle details of a twisted cylinder. Kukathasan and Pellegrino (2003) investigated the vibration behavior of large, ultra-lightweight membrane structures by using thin-shell elements in ABAQUS. Wong and Pellegrino (2002a; 2002b; 2003) studied the formation of wrinkles on thin membrane structures to obtain the detailed parameters of wrinkles, e.g., wavelength and amplitude. Leifer and Belvin (2003) performed similar numerical simulations using ANSYS. Tessler *et al*. (2003) carried out similar work at about the same time.

In this paper, the effects of the shear force, the prestress level, the boundary conditions, and the joint seam on wrinkle formation and evolution were studied.

2 Wrinkle criterion

A thin membrane can be in three different structural states: taut, wrinkled, or slack. According to the combined criterion (Junger, 1967; Jenkins *et al.*, 1998; Liu and Jenkins, 2000): when the second principal stress $\sigma_2>0$, the membrane is in a taut state; when the second principal stress $\sigma_2\leq 0$ and the first principal strain $\varepsilon_1>0$, the membrane is in a wrinkled state; when the first principal stress $\sigma_1\leq 0$ and the first principal strain $\varepsilon_1\leq 0$, the membrane is in a slack state.

Historically, most wrinkle formation studies were based on the assumption that the bending stiffness in the membrane can be neglected, and that wrinkles carry loads only in the direction of the major principal stress. However, Rimrott and Cvercko (1985) studied the critical compressive stress in a membrane, and revealed the effects of low bending stiffness and compressive minor principal stresses, both of which exist in a membrane that is subjected to in-plane compression body force.

All analyses in this study are based on the assumption that once a membrane has wrinkled, it is able to resist a small compressive stress, which varies only with the half-wavelength, λ, of the wrinkles and is equal to the critical buckling stress σ_{cr} of a simply-supported, infinitely wide thin plate in uniaxial compression, and can be given by Euler's formula

$$\sigma_{cr}=-\frac{\pi^2 Et^2}{12(1-\nu^2)\lambda^2}, \tag{1}$$

where E is Young's modulus, ν is Poisson's ratio, and t is the thickness of the membrane (Wong and Pellegrino, 2002a).

3 Finite element analysis

3.1 Modeling

The membrane structure analyzed here is a 250 mm×250 mm square membrane supported by top and bottom clamping frames. Its configuration and dimensions are given in Fig. 1, and the material properties are listed in Table 1. The membrane is Kapton HN100® film (Dupont, USA), the edge wires are made of poly-benzol-oxylene (PBO) (Toyobo, Japan), the frame is stainless steel plate, and the glue is a self-developed epoxy mixture, named Epo-bond, which was demonstrated successfully in previous studies.

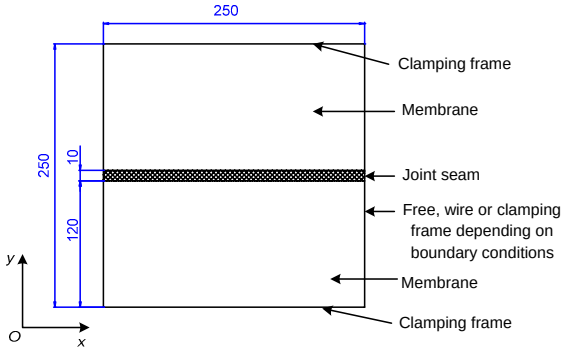

Fig. 1 Structure of the planar film reflect-array with a joint seam (unit: mm)

The commercial FE code ABAQUS 6.8 (Dassault Systems Simulia Corporation, USA) was used to simulate wrinkle behavior. Since membrane elements have zero bending stiffness, a shell element was chosen here. The element labeled S4R5 was selected based on its avoidance of parasitic locking, computational economy and accuracy compared with other kinds of shell elements (Wong and Pellegrino, 2006).

To allow the mesh to reveal wrinkles, the element size should be set to less than one half of the expected wrinkle wavelength, λ, which can be estimated from (Epstein, 2003; Wong and Pellegrino, 2003)

Table 1 Properties of the components

Component	Material	Density (kg/m^3)	Young's modulus (N/mm^2)	Poisson's ratio	Geometry dimension
Membrane	Kapton®	1500	3530	0.30	0.025 mm*
Wire	PBO®	1560	152900	0.30	0.12566 mm^{2**}
Frame	Steel	7930	205000	0.35	30 mm×30 mm**
Glue	Epo-bond	1090	400000	0.30	0.003 mm*

Material properties of the membrane were taken from Wong and Pellegrino (2002b), and those of the wire were taken from material property test report. The glue was a mixture of epoxy resin 618® and epoxy resin 650® in a ratio of 1:1 by weight, and its properties were estimated by taking consideration of experimental results from uniaxial tension of membrane tapes with glued joint bands. * Thickness; ** cross-section area

$$\lambda=\frac{\sqrt{\pi}}{[3(1-\nu^2)]^{1/4}}\frac{\sqrt{xt}}{\gamma^{1/4}}, \tag{2}$$

where $\gamma=\delta/L$, δ is the horizontal small displacement applied to the top edge of the membrane structure, L is the length of the square membrane structure, and x is the horizontal position of the wrinkle.

Substitution of the involved parameters, x= 10 mm, t=0.025 mm, ν=0.3, and γ=0.15/250, of the structure in this study into Eq. (2), gave λ=3.427 mm. After considering factors such as the chosen shell element type, the desire to resolve corner wrinkles, and the capacity of computation, a 1 mm square element was chosen.

The top and bottom clamping frames were modeled by the beam element labeled B21 beam elements (Wong and Pellegrino, 2002b) and clamping frames were applied to the vertical membrane edges. Wires applied to the vertical edges were modeled by the truss element labeled T3D2 truss elements. When studying the effect of the joint seam, the glue was modeled by the solid element labeled C3D8R solid elements.

3.2 Analysis

The simulation consists of three main parts, namely, setting up an initial, lightly prestressed membrane, an eigenvalue analysis leading to the imperfection modes that will be seeded into the membrane, and a post-wrinkling analysis with numerical stabilization.

Two kinds of methods were used here to introduce prestress into the membrane. One was to tension the membrane by applying some displacement to the top edge in the y-direction. When doing so, translation in only the y-direction was allowed for the two side edges, and all six degrees of freedom of the bottom edge were completely constrained. The second method was to use the "*INITIAL CONDITIONS, TYPE=STRESS" parameter in ABAQUS. The geometric stiffness provided by the prestress has the effect of increasing the out-of-plane stiffness of the thin membrane.

In the second step, the Lanczos method was used to carry out the eigenvalue analysis using the "EIGENSOLVER=LANCZOS" parameter in the "*BUCKLE" option. Some selected global deformation modes were combined, and introduced into the structure as a geometrical imperfection. The imperfection was defined through the "IMPERFECTION" option provided by ABAQUS:

$$\Delta z=\sum_i \omega_i\phi_i, \tag{3}$$

where ϕ_i is the ith eigenmode, and ω_i is a scaling factor whose magnitude is chosen as a proportion of the thickness of the membrane. Here the value of ω_i was set to 25% of the thickness throughout the simulation.

The third and final step was a geometrical nonlinear "*NLGEOM" incremental analysis. Prestress is also needed to provide a small, initial out-of-plane stiffness to the membrane, but the value should be set small enough so that the final results are not affected. The "STABILIZE" function was activated for this step (Wong and Pellegrino, 2002b).

3.3 Results and discussion

3.3.1 Shear force effects and experimental validation

In the ABAQUS simulation, the prestress on the membrane was set to 0.1 N/mm^2, the two side edges of the membrane were free, and there was a glued horizontal joint seam in the center of the structure. There are two datasets in Table 2 that describe membrane structure's surface deformation characteristics.

One set is about the wrinkle pattern along structure's diagonal, and the other is the statistic data about the membrane's displacement in *z*-direction. When the shear displacement increased from 0.005 to 2.3 mm, the quantity of wrinkles increased from 3.5 to 6.5, and the average amplitude which is the distance between wrinkle's crest and its trough increased from 0.0212 to 2.33 mm. The membrane surface beside the two side edges became more uneven. When the shear displacement was only 0.005 mm, the quantity of wrinkles was 4, and the maximum amplitude which is the distance between Max-z and Min-z in the membrane was only 0.0247 mm. This may be because the shear force was too small to generate a complete set of wrinkles. Under such a low force, the structure did not completely buckle. The wave pattern of the membrane showed only the original imperfection added to the structure at the beginning of the analysis.

To validate the ABAQUS simulation method, an experiment was set up, and a series of tests of wrinkle patterns under different shear displacements was carried out (Fig. 2). The tension displacement of the membrane top edge was 0.5 mm. The total shear displacement of the top clamping frame was varied from 0.6 to 3.1 mm.

In the ABAQUS simulation, the thickness of the glue layer was set to 3 μm, so the joint band had a significant influence on the wrinkle pattern of the structure (Fig. 2c). In the experiment, the glue layer was paved and extruded extremely thinly to ensure a reliable joint between the two pieces of membrane. As it may have been only several tenths of a micron, the joint band had no obvious effect on the wrinkle pattern of the structure (Figs. 2a and 2b). This situation is discussed in detail in Section 3.3.4. Apart from this, the experimental results revealed the same

Table 2 Surface deformation characteristics under different shear force levels

Shear displacement (mm)	Wrinkle's quantity	Average amplitude (mm)	Max-*z* (mm)	Min-*z* (mm)	*E*(*z*) (mm)	*D*(*z*)/RMS (mm)
0.0050	4	0.0212	0.1268	−0.1204	5.79×10^{-5}	0.00835
0.015	3.5	0.251	0.2431	−0.1497	2.88×10^{-4}	0.0634
0.030	3.5	0.413	0.3311	−0.2439	−0.00318	0.111
0.075	3.5	0.641	0.4894	−0.3211	0.00351	0.167
0.15	4	0.795	0.6166	−0.4138	−0.00263	0.220
0.35	5	1.02	0.8255	−0.7276	0.00530	0.326
0.75	6	1.19	1.341	−1.363	−0.00186	0.444
1.55	6.5	1.61	1.566	−1.092	0.02410	0.577
2.30	6.5	2.33	1.136	−2.583	−0.18000	0.827

Max-*z* and Min-*z* are the maximum and minimum *z*-direction displacements in the membrane, respectively; *E*(*z*) is the mean *z*-direction displacement; and *D*(*z*)/RMS is the root mean square of the *z*-direction displacement

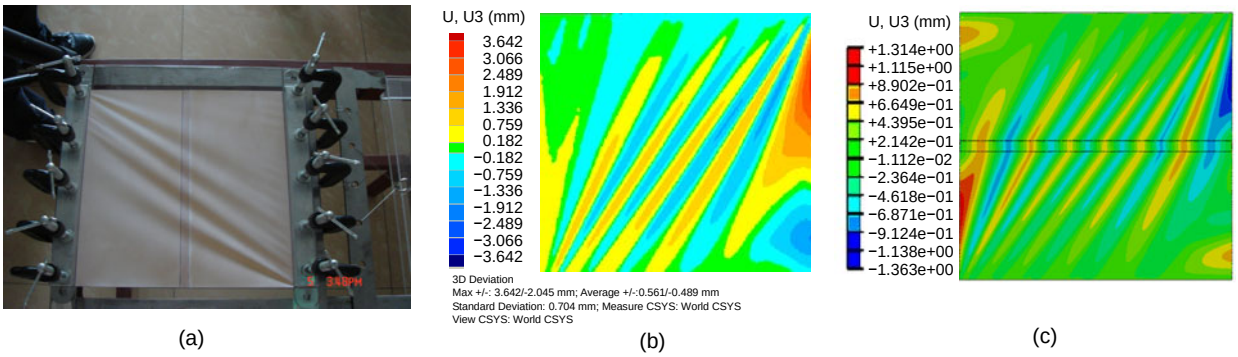

(a) (b) (c)

Fig. 2 *z*-direction displacement of the structure under shear displacement force

(a) Experimental set-up and a wrinkle pattern photograph of the structure taken on site (the Kapton® film is covered with a very thin layer of high diffusion reflective white material); (b) *z*-direction displacement contour of the structure converted with an image modeler (shear displacement, 1.6 mm); (c) *z*-direction displacement contour of the structure in the ABAQUS simulation (shear displacement, 0.75 mm)

wrinkle characteristics as the ABAQUS simulation.

In an experimental situation, clamping frames are not totally rigid, clamp tools cannot clamp the membrane absolutely firm, there is clearance between experimental parts, and it is not easy to control the prestress in the membrane precisely. As a result of these factors, the shear displacement values in the experiment do not correspond exactly to those in the ABAQUS simulation. Thus, there is a deviation between the experimental result curve and the simulation result curve. But the development of these two curves is the same, as shown clearly in Figs. 3 and 4. Since it was difficult to perform a successful test under a shear displacement of less than 0.5 mm in this experiment, and the analysis was not convergent under a shear displacement of more than 2.5 mm in this series of simulations, no low end experimental result or high end simulation result is shown in the figures.

3.3.2 Prestress effects

The two side edges of the membrane were free and the membrane was made of one whole piece without joint seams. The total shear displacement of the top clamping frame was 1.2 mm. Fig. 5 shows the *z*-direction displacement contour of the structure under a prestress of 0.5 N/mm^2.

As shown in Table 3, when the prestress was increased from 0.01 to 2.0 N/mm^2, the quantity of wrinkles generated in the middle part of the membrane rose from 4.5 to 6, and the average amplitude gradually dropped by about one third. The membrane surfaces along the two side edges became smoother with increasing prestress (Fig. 6). This can be seen

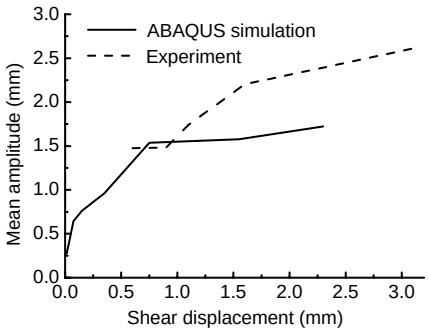

Fig. 4 Wrinkle amplitude curves of experimental and ABAQUS simulation results

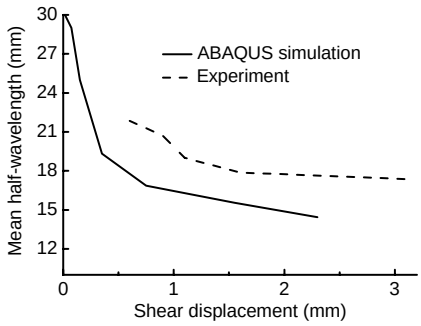

Fig. 3 Wrinkle half-wavelength curves of experimental and ABAQUS simulation results

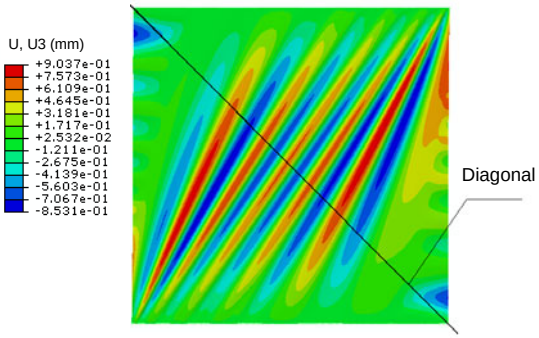

Fig. 5 *z*-direction displacement of the structure under a prestress of 0.5 N/mm^2

Table 3 Surface deformation characteristics under different prestress levels

Prestress level (N/mm^2)	Wrinkle's quantity	Average amplitude (mm)	Max-*z* (mm)	Min-*z* (mm)	*E*(*z*) (mm)	*D*(*z*)/RMS (mm)
0.01	4.5	1.56	0.9544	−1.008	−0.0744	0.414
0.05	5	1.37	1.218	−1.266	0.0903	0.402
0.1	5	1.27	1.091	−1.087	6.16×10^{-5}	0.393
0.2	5.5	1.20	1.084	−0.8401	0.0108	0.380
0.3	5.5	1.15	0.9824	−0.8944	-2.16×10^{-4}	0.386
0.5	5.5	1.11	0.9037	−0.8531	−0.0604	0.358
1.0	5.5	1.08	0.8892	−0.8182	0.00327	0.334
2.0	6	1.06	0.8374	−0.8181	0.0120	0.301

Max-*z* and Min-*z* are the maximum and minimum *z*-direction displacements in the membrane, respectively; *E*(*z*) is the mean *z*-direction displacement; and *D*(*z*)/RMS is the root mean square of the *z*-direction displacement

clearly at the two ends of the wrinkle curves, which became much flatter as the prestress increased. The whole membrane surface also became smoother, shown by the reduction in the $D(z)$/RMS. However, the wrinkle pattern generated under a prestress of 0.01 N/mm^2 did not accord with this trend completely. This may be because such a prestress is too low to tensioning the membrane sufficiently.

3.3.3 Boundary condition effects

For this set of simulations, the prestress on the membrane was set to 0.1 N/mm^2 and the membrane was one whole piece without joint seams. The total shear displacement of the top clamping frame was 1.2 mm. Three kinds of side edge supports were considered here: free-side-edge, wire-side-edge, and frame-side-edge. For wire-side-edge support, four specific kinds of edge wire conditions were studied: straight-side-wire, tied-circle-side-wire, slide-circle-side wire, and all-tied-circle-wire.

As shown in Figs. 7–9, the structure of frame-side-edge generated the largest quantity of wrinkles, and that quantity was much larger than those of the other two side edge forms which generated an almost identical wrinkle state. When the structure had the frame-side-edge, the wrinkle amplitude decreased to about one-half of that of the other support conditions. In the middle section of the membrane, the free-side-edge structure and the wire-side-edge structure had nearly the same wrinkle pattern, but in the area beside the side edge, the free-side-edge structure had several horizontal wrinkles which were parallel to the shear force direction. For the wire-side-edge structure, however, there were no such wrinkles, so it had a much smoother surface than the free-side-edge structure in this part of the membrane.

Table 4 shows that the maximum von Mises stresses of both the wire-side-edge structure and the free-side-edge structure were nearly three times higher than those of the frame-side-edge structure, but they existed only in a very small area near the corner. Across the majority of the membrane, the von Mises stresses of both the wire-side-edge and free-side-edge structures were much smaller. All three structures with circle edge wire support had better wrinkle performance than any of the structures with straight wire support. Among them, the slide-circle-side-wire structure had the lowest maximum wrinkle amplitude, but it had the most uneven stress distribution. The all-tied-circle-wire structure had the most even

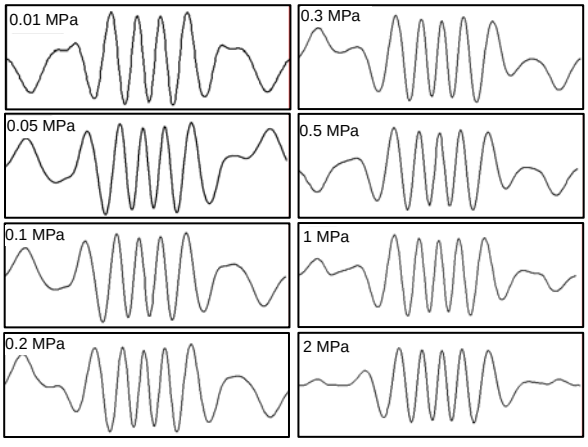

Fig. 6 Wrinkle pattern along the diagonal of the membrane under different prestress levels

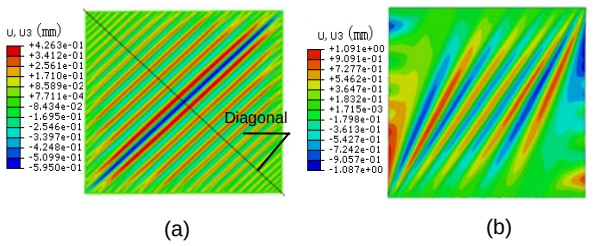

Fig. 7 z-direction displacement of the structure with different side-edge supports

(a) Frame-side-edge; (b) Free-side-edge

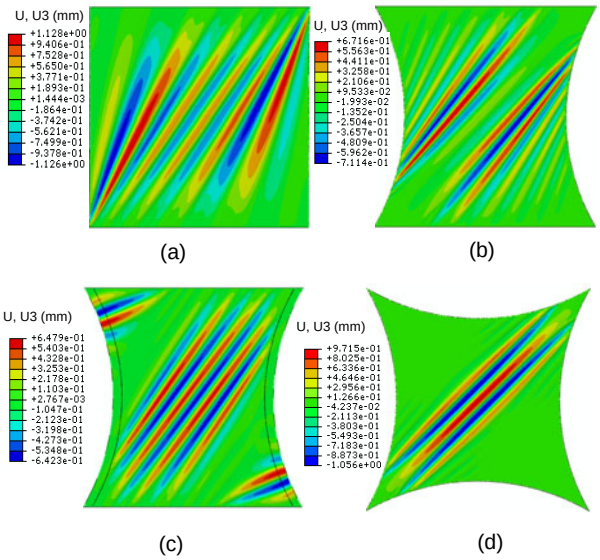

Fig. 8 z-direction displacement of the structure under different edge wire conditions

(a) Straight-side-wire; (b) Tied-circle-side-wire; (c) Slide-circle-side-wire; (d) All-tied-circle-wire

stress distribution, but its wrinkle amplitude was relatively high. When taking both aspects into consideration, the tied-circle-side-wire structure had the best combined performance.

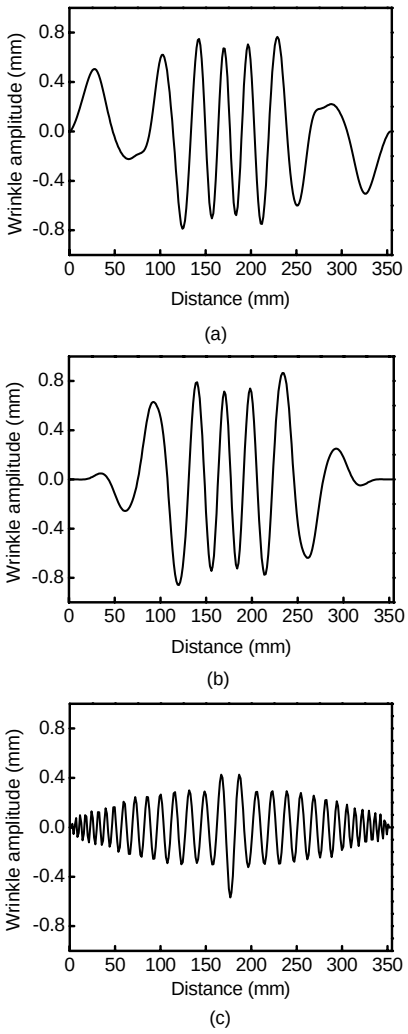

Fig. 9 Wrinkle pattern along the diagonal of the membrane with different side-edge supports
(a) Free-side-edge; (b) Wire-side-edge; (c) Frame-side-edge

3.3.4 Influence of the joint seam

For this set of simulations, the prestress on the membrane was 0.1 N/mm^2 and the two side edges of the membrane were free. The total shear displacement of the top clamping frame was 2.3 mm. Three approaches were used to simulate the joint seam. One was to neglect it by treating the structure as though it were made of a single piece of membrane. The second was to consider that there was only an overlapping band of membrane material. The third was to take full consideration of a glue band between the two pieces of membrane. A structure with a fully considered glued joint seam perpendicular to the shear force direction was also studied.

As shown in Fig. 10 and Table 5, the structure with a horizontal joint seam had the most uneven surface. The structure with a perpendicular joint seam had a little higher maximum wrinkle amplitude, but its surface was the most even. The other two structures had almost the same wrinkle pattern.

For the horizontal joint seam structure (Fig. 10c), there were significant wrinkle pattern changes within and beside the joint seam. The wrinkles showed two turns, one on either side of the joint seam. The turn on the top side was anticlockwise, while the turn on the bottom side was clockwise. Within the joint seam, the wrinkles ran almost vertically. After passing through the seam, the wrinkles returned to their original directions, but with a small excursion in the *x*-direction. For the vertical joint seam structure (Fig. 10d), the wrinkle patterns beside the joint seam were also greatly altered. The wrinkles in the two half membranes did not expand continuously. There were no obvious wrinkles within the joint seam. The joint seam revealed distinct anisotropic wrinkle characteristics under shear force action. In the area beside the

Table 4 Surface deformation and stress characteristics under different boundary conditions

Boundary condition	Wrinkle's quantity	Max-σ (N/mm^2)	Min-σ (N/mm^2)	Max-z (mm)	Min-z (mm)	$E(z)$ (mm)	$D(z)$/RMS (mm)
Free-side-edge	5.5	62.73	1.205×10^{-2}	1.091	−1.0870	6.16×10^{-5}	0.3930
Frame-side-edge	30	20.22	14.29	0.4263	−0.5950	-1.55×10^{-3}	0.1890
Straight-side-wire	6	70.72	0.1450	1.128	−1.1260	1.45×10^{-5}	0.1850
Tied-circle-side-wire	15	19.14	0.9389	0.6716	−0.7114	6.08×10^{-3}	0.0506
Slide-circle-side-wire	6	123.4	2.302×10^{-4}	0.6479	−0.6423	4.25×10^{-3}	0.0662
All-tied-circle-wire	3	12.99	1.208	0.9715	−1.0560	2.93×10^{-3}	0.0971

Max-σ and Min-σ are the maximum and minimum von Mises stress in the membrane, respectively; Max-*z* and Min-*z* are the maximum and minimum *z*-direction displacements in the membrane, respectively; $E(z)$ is the mean *z*-direction displacement; and $D(z)$/RMS is the root mean square of the *z*-direction displacement

Table 5 Surface deformation characteristics under different joint seam treatments

Joint seam condition	Wrinkle's quantity	Max-*z* (mm)	Min-*z* (mm)	*E*(*z*) (mm)	*D*(*z*)/RMS (mm)
One piece	6	1.164	−1.127	0.0822	0.610
Membrane material overlapping	6	1.127	−1.163	−0.0812	0.611
Horizontal joint seam	6.5	1.136	−2.583	−0.1800	0.827
Vertical joint seam	6	1.292	−1.294	−0.0883	0.165

Max-*z* and Min-*z* are the maximum and minimum *z*-direction displacements in the membrane, respectively; *E*(*z*) is the mean *z*-direction displacement; and *D*(*z*)/RMS is the root mean square of the *z*-direction displacement

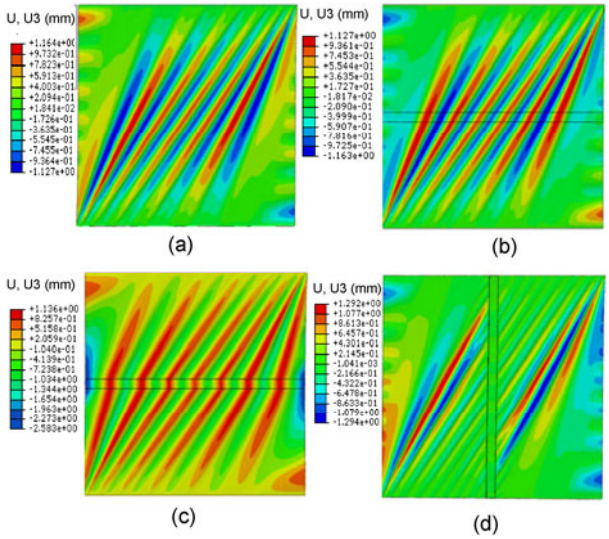

Fig. 10 *z*-direction displacement contours of the structures under different conditions of the joint seam
(a) One piece; (b) Membrane material overlapping; (c) Horizontal joint seam; (d) Perpendicular joint seam

side edges, there were several horizontal waves in the one piece structure, the overlapping membrane structure, and the structure with a perpendicular joint seam. For the structure with a horizontal joint seam, there was only one horizontal wave, but its amplitude was a little higher.

4 Conclusions

A numerical analysis method was used to simulate wrinkle emergence and propagation in a planar film reflect-array. Some characteristic parameters were obtained. The boundary conditions, prestress level, joint seam and shear displacement all had important effects on the wrinkle pattern of the planar film reflect-array. Designing a rational membrane boundary and producing a rational tension distribution in the membrane are the key factors controlling the wrinkles on a planar film reflect-array.

The effects on the membrane wrinkle pattern of other factors, such as the properties and the prestress of the edge wire, the shape of the edge curve (circle, parabola), and the properties of the joint seam (width, thickness and glue properties), will be studied in future work.

References

Adler, A.L., Mikulas, M.M., 2000. Static and Dynamic Analysis of Partially Wrinkled Membrane Structures. Proceedings of the 41st AIAA/ASME/ASCE/AHS/ASC Structures, Structural Dynamics, and Material Conference and Exhibit, Atlanta, GA., AIAA-2000-1810.

Calladine, C.R., 1983. Theory of Shell Structures. Cambridge University Press, Cambridge, England.

Epstein, M., 2003. Differential equation for the amplitude of wrinkles. *AIAA Journal*, **41**(2):327-329. [doi:10.2514/2.1952]

Greschik, G., Mikulas, M.M., 2001. Design Study of a Square Sail Architecture. Proceedings of the 42nd AIAA/ASME/ASCE/AHS/ASC Structures, Structural Dynamics, and Material Conference and Exhibit, Seattle, WA, USA, AIAA-2001-1259.

Jenkins, C.H., Haugen, F., Spicher, W.H., 1998. Experimental measurement of wrinkling in membranes undergoing planar deformation. *Experimental Mechanics*, **38**(2):147-152. [doi:10.1007/BF02321658]

Johnston, J.D., 2002. Finite Element Analysis of Wrinkled Membrane Structures for Sunshield Applications. Proceedings of the 43rd AIAA/ASME/ASCE/AHS/ASC Structures, Structures Dynamics, and Material Conference and Exhibit, Denver, CO, USA, AIAA-2002-1369.

Junger, M.C., 1967. Normal Modes of Submerged Plates and Shells. Symposium on Fluid-Solid Interaction, ASME, p.95.

Kukathasan, S., Pellegrino, S., 2003. Nonlinear Vibration of Wrinkled Membranes. Proceedings of the 44th AIAA/ASME/ASCE/AHS/ASC Structures, Structures Dynamics, and Material Conference and Exhibit, Norfolk, VA, USA, AIAA-2003-1745.

Lai, C.Y., 2001. Analysis and Design of a Deployable Membrane Reflector. PhD Thesis, University of Cambridge, Cambridge, England.

Leifer, J., Belvin, W.K., 2003. Prediction of Wrinkle Amplitudes in Thin Film Membrane via Finite Element Modeling. Proceedings of the 44th AIAA/ASME/ASCE/AHS/ASC Structures, Structural Dynamics, and Material Conference and Exhibit, Norfolk, VA, USA, AIAA-2003-1982.

Liu, X., Jenkins, C.H., 2000. Fine scale analysis of wrinkled membranes. *International Journal of Computational Engineering Science*, **1**(2):281-298. [doi:10.1142/S1465876300000148]

Mansfield, E.H., 1968. Tension Field Theory, a New Approach which Shows its Duality with Inextensional Theory. Proceedings of the 12th International Congress of Applied Mechanics, Stanford, CA, USA, p.305-320.

Mansfield, E.H., 1970. Load transfer via a wrinkled membrane. *Proceedings of The Royal Society A: Mathematical Physical and Engineering Sciences*, **316**(1525):269-289. [doi:10.1098/rspa.1970.0079]

Miller, R.K., Hedgepeth, J.M., 1985. Finite element analysis of partly wrinkled membranes. *Computers and Structures*, **20**(1-3):631-639. [doi:10.1016/0045-7949(85)90111-7]

Mseikeh, C.H., 1997. Wrinkling of Membranes, Plates, and Shells. PhD Thesis, McGill University, Quebec, Canada.

Pipkin, A.C., 1986. The relaxed energy density for isotropic elastic membrane. *IMA Journal of Applied Mathematics*, **36**(1):85-99. [doi:10.1093/imamat/36.1.85]

Rimrott, F.P.J., Cvercko, M., 1985. Wrinkling in Thin Plates Due to In-Plane Body Forces. *In*: Bevilacqua, L., Feijoo, R., Valid, R. (Eds.), Inelastic Behavior of Plates and Shells, Springer-Verlag, Berlin, Germany, p.19-48.

Steigmann, D.J., Pipkin, A.C., 1989a. Finite deformations of wrinkled membranes. *Quarterly Journal of Mechanics and Applied Mathematics*, **42**(3):427-440. [doi:10.1093/qjmam/42.3.427]

Steigmann, D.J., Pipkin, A.C., 1989b. Wrinkling of pressurized membranes. *Journal of Applied Mechanics*, **56**(3):624-628. [doi:10.1115/1.3176137]

Stein, M., Hedgepeth, J.M., 1961. Analysis of Partly Wrinkled Membranes. NASA TN D-813.

Tessler, A., Sleight, D.W., Wang, J.T., 2003. Nonlinear Shell Modeling of Thin Membrane with Emphasis on Simulation Wrinkling. Proceedings of the 44th AIAA/ASME/ASCE/AHS/ASC Structures, Structural Dynamics, and Material Conference and Exhibit, Norfolk, VA, USA, AIAA-2003-1931.

Wong, Y.W., Pellegrino, S., 2002a. Amplitude of Wrinkles in Thin Membrane. *In*: Drew, H., Pellegino, S. (Eds.), New Approaches to Structural Mechanics, Shells and Biological Structures. Kluwer Academic Publishers, London, UK, p.257-270.

Wong, Y.W., Pellegrino, S., 2002b. Computation of Wrinkle Amplitudes in Thin Membrane. Proceedings of the 43rd AIAA/ASME/ASCE/AHS/ASC Structures, Structural Dynamics, and Material Conference and Exhibit. Denver, CO, USA, AIAA-2002-1369.

Wong, Y.W., Pellegrino, S., 2003. Prediction of Wrinkle Amplitude in Square Solar Sails. Proceedings of the 44th AIAA/ASME/ASCE/AHS/ASC Structures, Structural Dynamics, and Material Conference and Exhibit, Norfolk, VA, USA, AIAA-2003-1982.

Wong, Y.W., Pellegrino, S., 2006. Wrinkled membrane, Part III: Numerical simulations. *Journal of Mechanics of Materials and Structures*, **1**(1):61-93.